

Role of a low-viscosity zone in stabilizing plate tectonics: Implications for comparative terrestrial planetology

Mark A. Richards

Department of Earth and Planetary Science, University of California, Berkeley, California 94720, USA
(markr@seismo.berkeley.edu)

Woo-Sun Yang

Institute of Geophysics and Planetary Physics, Los Alamos National Laboratory, Los Alamos, New Mexico 87545, USA (wyang@lbl.gov)

John R. Baumgardner

Theoretical Division, Los Alamos National Laboratory, Los Alamos, New Mexico 87545, USA
(baumgardner@lanl.gov)

Hans-Peter Bunge

Department of Geosciences, Princeton University, Princeton, New Jersey 08540, USA (bunge@Princeton.edu)

[1] **Abstract:** Earth's near-surface layer, its lithosphere, is broken into quasi-rigid plates that form the upper thermal boundary layer for mantle convection. Since the discovery of plate tectonics, it has been widely conjectured but only recently demonstrated that this peculiar style of convection may be facilitated by an upper mantle low viscosity zone (LVZ) over which the plates glide easily. The LVZ, or "asthenosphere," concept dates from 19th century investigations of isostatic support of mountain belts and is supported by modern evidence for a seismic low velocity zone and by studies of postglacial rebound and dynamic compensation of the Earth's gravity field. Here we show in both two-dimensional (2-D) Cartesian and 3-D spherical Earth models that combining a pronounced LVZ and a plastic yield stress to allow localized weakening of the cold thermal boundary layer results in a distinctly plate tectonic style of convection, with ~30% toroidal surface motion for the 3-D case. Recycling of water into the upper mantle at subduction zones is a plausible cause of Earth's LVZ, whereas Venus is dry and lacks both an LVZ and plate tectonics.

Keywords: Plate tectonics; mantle convection; mantle viscosity; rheology; Venus; lithosphere.

Index terms: Dynamics of lithosphere and mantle—general; planetary tectonics; plate motions—general; rheology—mantle.

Received October 18, 2000; **Revised** February 19, 2001; **Accepted** April 3, 2001; **Published** August 23, 2001.

Richards, M. A., W.-S. Yang, J. R. Baumgardner, and H.-P. Bunge, 2001. Role of a low-viscosity zone in stabilizing plate tectonics: Implications for comparative terrestrial planetology, *Geochem. Geophys. Geosyst.*, vol. 2, Paper number 2000GC000115 [3948 words, 5 figures, 1 appendix table]. Published August 23, 2001.

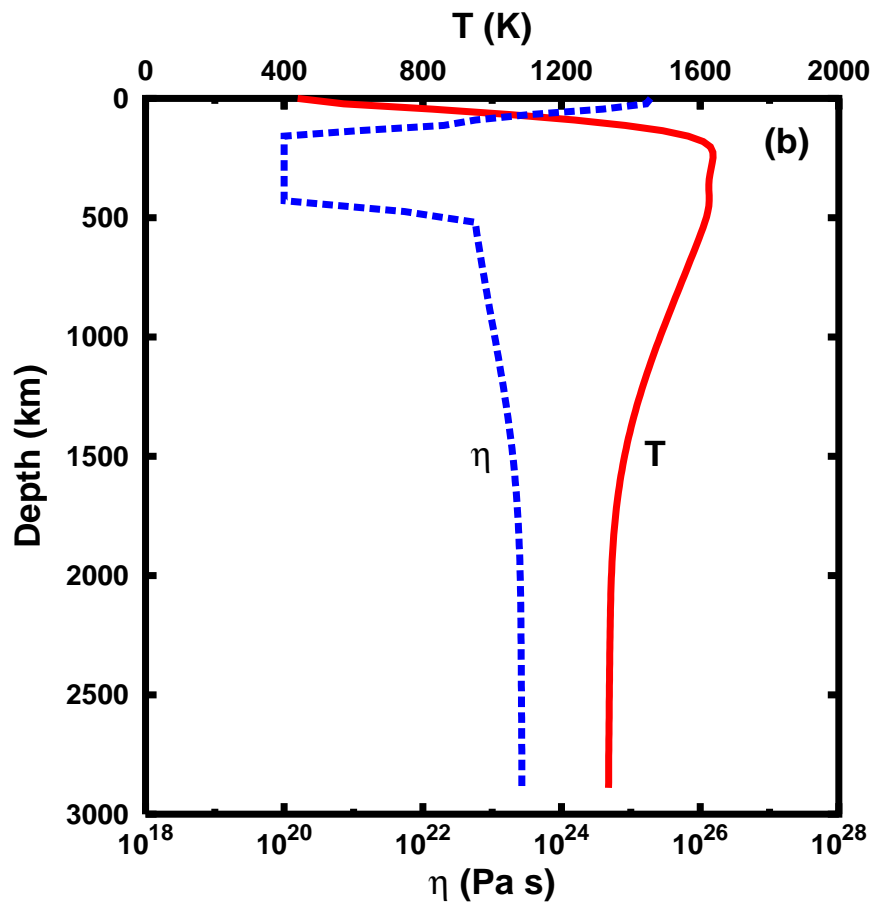
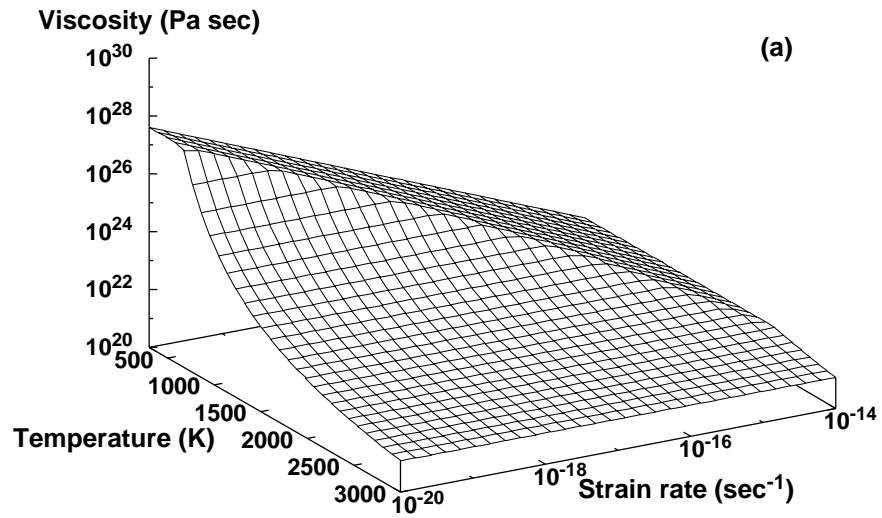
1. Introduction

[2] A low viscosity zone (LVZ) separating the base of the lithosphere from the deeper mantle has been postulated on the basis of a variety of evidence [see, e.g., *Cathles*, 1975; *Hager and Richards*, 1989; *Mitrovica*, 1996], and this rheological LVZ is probably related to the seismic “low velocity zone” found beneath oceanic and tectonically active regions at depths of 100–300 km [e.g., *Hales et al.*, 1968; *Grand and Helmlinger*, 1984]. The role of an LVZ in regulating or promoting plate tectonics has not previously been systematically investigated in full convection models, because geodynamicists have only recently achieved the capability to simulate extreme viscosity contrasts and shear failure in the lithosphere. Using a new numerical modeling technique well suited to this challenge [*Yang and Baumgardner*, 2000], we investigate here an important and straightforward question: Given a reasonable failure mechanism for the lithosphere, does an LVZ facilitate a plate tectonic style of mantle convection?

[3] Plate treatment persists as a serious challenge to mantle convection modelers, because it is difficult to simulate shear failure at plate boundaries. Approaches include highly nonlinear (non-Newtonian) viscous creep [*Weinstein and Olson*, 1992], prescribed frictional faults, strain rate weakening rheologies, and viscoplastic yielding [*Bercovicci*, 1993; *Zhong et al.*, 1998; *Tackley*, 2000b] (see also *King et al.* [1992] for a comparison of several methods for numerical simulation of plates in mantle convection models). *Moresi and Solomatov* [1998] recently explored the effects of strongly temperature dependent viscosity combined with a plastic yield stress: the former causes the cold upper boundary layer (lithosphere) to be strong, while the latter allows this

boundary layer to fail locally in regions of high stress. *Moresi and Solomatov* [1998] identified three styles of convection similar to those described earlier by *Weinstein and Olson* [1992] for non-Newtonian lithospheric behavior: (1) a “frozen lid” regime at high yield stress in which the cold upper boundary layer is immobile, (2) a “mobile lid” regime at low yield stress in which ubiquitous plastic failure of the lithosphere yields a continuously mobile upper boundary layer, and (3) a “transitional” regime that switches episodically between the frozen and mobile regimes. Regime 1 appears applicable to Mars (a “one-plate” planet) and the Moon, while regime 3 may describe the distributed deformation and episodic overturn of Venus’ lithosphere [*Strom et al.*, 1994; *Weinstein*, 1996a, 1996b; *Moresi and Solomatov*, 1998]. However, no stable plate-like (Earth-like) regime was identified.

[4] Three-dimensional mantle convection models show that a low-viscosity upper mantle promotes convection in a few large elongated cells bounded by a network of linear downwellings [*Bunge et al.*, 1996]. This discovery suggests that a sublithospheric LVZ might stabilize a plate-like convection regime in the system explored by *Moresi and Solomatov* [1998]; specifically, a regime in which the horizontal motions of the upper boundary layer are stable, piecewise-constant, and separated by narrow zones of high rates of strain. Further indications that this might be so come from mechanical models of plates that show that one needs an LVZ in order for lithosphere to remain plate-like near fault zones [*Zhong et al.*, 1998]. Here we demonstrate that an LVZ acts strongly to stabilize plate tectonics, first exploring model parameter space with computationally less demanding two-dimensional (2-D) models, and then demonstrating similar plate-like behavior in 3-D spherical calculations.



2. Methods

[5] We use a matrix-dependent transfer multigrid method [Alcouffe *et al.*, 1981; Yang and Baumgardner, 2000] to solve the momentum equation with strong spatial variations in viscosity. The 2-D models are executed in a long box of 4×1 aspect ratio (512×128 cells) that is internally (radioactively) heated, cooled from the top, and insulated at the bottom, with free-slip top and bottom boundaries and wraparound end boundary conditions. Earth-like values are used for mantle depth (2890 km), density (3400 kg/m^3), thermal expansivity ($2.5 \times 10^{-5}/\text{K}$), thermal conductivity (4 W/m-K), specific heat (1000 J/kg-K), and radioactive heating ($5 \times 10^{-12} \text{ W/kg}$).

[6] We use a strongly temperature-dependent Newtonian-viscous/perfectly plastic rheological law with an activation energy of 100 kJ/mole, a mantle-averaged viscosity consistent with postglacial rebound studies [Cathles, 1975; Mitrovica, 1996], and a plastic yield stress that we vary in this study. The activation energy used here is reduced about a factor of 5 from laboratory values [Karato and Wu, 1993] but still produces 6 orders of magnitude in viscosity variation over the temperature range of the models. In a classic study, Christensen [1984] showed that the combination of non-

Newtonian ($n = 3$) power law rheology combined with more realistic activation energies results in convection resembling Newtonian convection with activation energies similar to that used here. For the present purpose of studying the effects of an LVZ, Newtonian rheology with a reduced activation energy is an appropriate approach.

3. Cartesian 2-D Results

[7] Figure 1a shows a map of viscosity versus temperature and strain rate for a lithospheric yield stress of 80 MPa. High strain rates lead to low effective viscosity and local reduction of the effect of cold temperature in the upper boundary layer, giving rise to shear failure in the lithosphere above mantle upwellings and downwellings.

[8] We introduce an LVZ in our models by prescribing an interval of reduced viscosity, perhaps caused by the presence of volatiles, probably water [Hirth and Kohlstedt, 1996; Karato and Jung, 1998], just below the thermal boundary layer (Figure 1b). When the mantle geotherm (solid red line) exceeds a temperature that represents the lower extent of the lithosphere, viscosity is reduced by a factor of 100. This low viscosity continues to an arbitrary cutoff depth of 500 km, at which point the

Figure 1. (a) Map of viscosity versus temperature and strain rate for a Newtonian (linear) viscous fluid with exponential dependence of viscosity upon temperature and a plastic yield stress of $\sigma_y = 80 \text{ MPa}$. One may consider the lithosphere to be pervasively faulted, so that frictional slip may occur in any orientation when a characteristic fault strength, or yield stress, is exceeded. When the local second stress invariant exceeds the yield stress, the local viscosity is reduced until the local stress is reduced to the yield stress value (thus decreasing the local strain rate.) Otherwise, viscosity is proportional to $\exp(E/RT)$, where the activation energy E is 100 kJ/mole, R is the ideal gas constant, and T is temperature. This results in ~ 6 orders of magnitude viscosity contrast across the full range of temperatures in the convection models. (b) Temperature (solid red line) and viscosity (dotted blue line) versus depth in the mantle for a vertical profile about halfway between upwelling and downwelling structures in Figure 2b. Viscosity is reduced by a factor of 100 when the temperature reaches a value characteristic of the base of the lithosphere. This reduction is maintained to a depth of 500 km, at which point the viscosity increases by a factor of $\eta^* = 1000$. The reference viscosity in each calculation is adjusted to maintain an overall mantle viscosity consistent with postglacial rebound values [Cathles, 1975; Mitrovica, 1996].

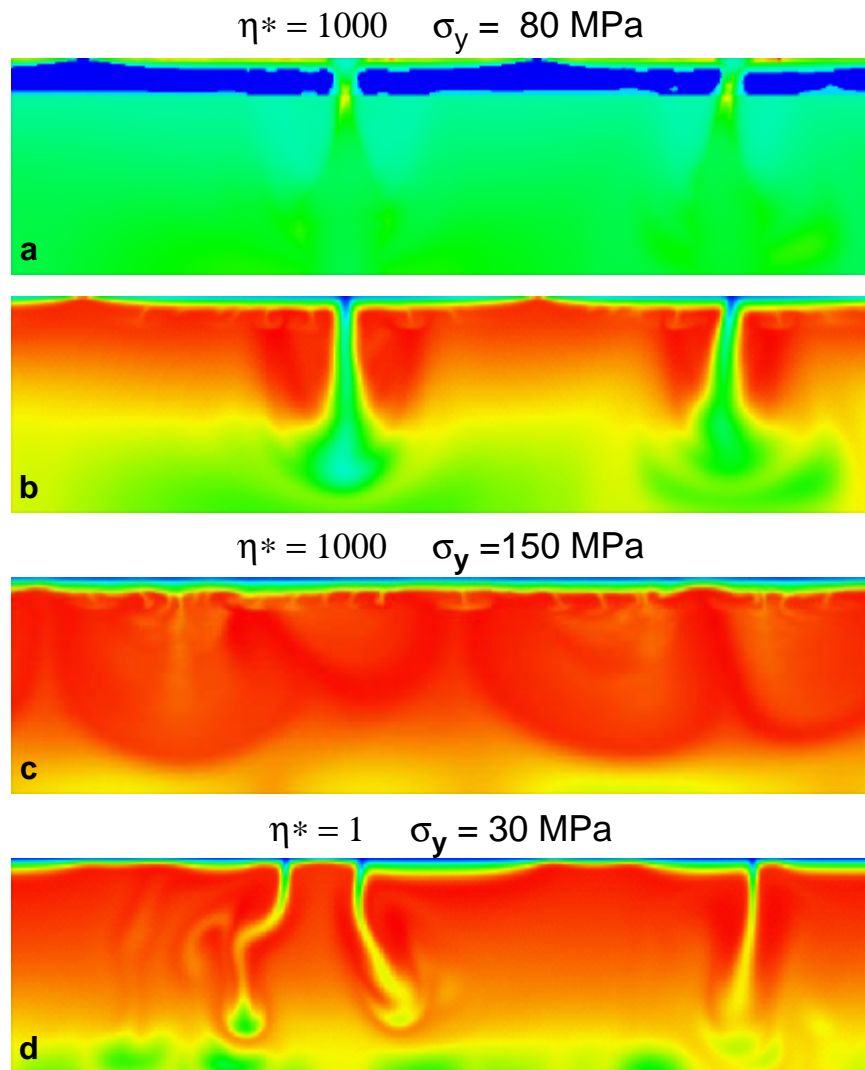


Figure 2. (a) Log viscosity for the plate-like case, with blue representing low viscosity (10^{20} Pa s) and red high viscosity (1.3×10^{28} Pa s). The LVZ is interrupted by two large cold downwellings, and it intrudes near the surface at the two major upwellings. (b) Temperature for the plate-like case, with blue cold (44°C) and red hot (1437°C). Note the slightly subadiabatic lower mantle fed by two large, stable downwelling structures. (c) Temperature for the frozen lid case. Note the pervasive small-scale convection beneath the immobile lithosphere. (d) Temperature for the mobile lid case. The thermal heterogeneity structure reflects downwellings that are very unstable in time or chaotic.

viscosity increases by a factor of η^* , which we vary from 1 to 10,000, resulting in a “notch” in the viscosity curve (dotted blue line, Figure 1b). This procedure for introducing an LVZ has the advantage of allowing low viscosity to

intrude naturally to shallow depths beneath warm upwelling zones while preserving the high viscosity of cold downwellings. We have found that weakening beneath ridges (perhaps due to partial melting) is important in promot-

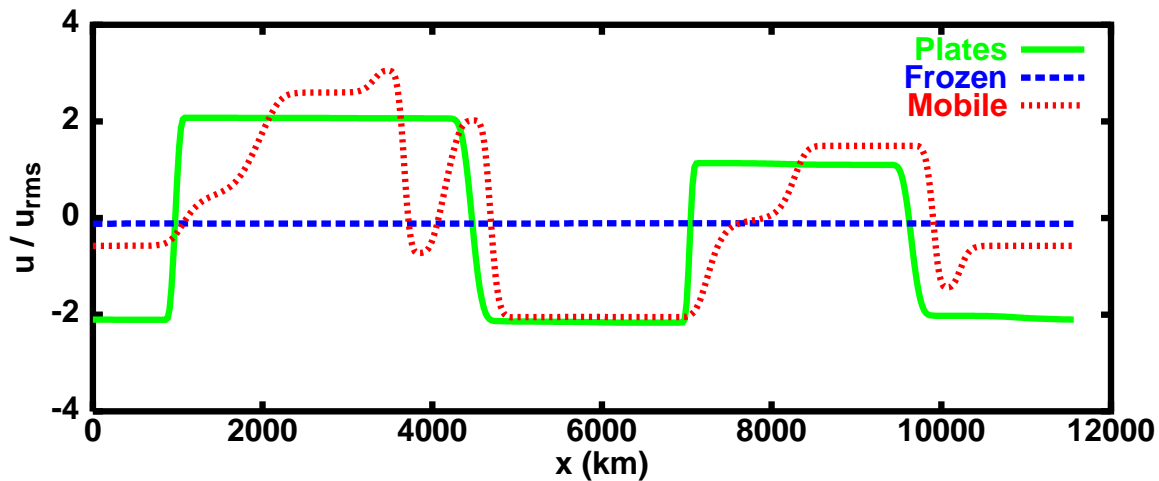


Figure 3. Horizontal surface velocity profiles for the plate-like (solid green line), frozen lid (dashed blue line), and mobile lid (dotted red line) cases. Horizontal velocities are normalized by the average horizontal velocity of the mantle interior. This normalization clearly distinguishes the frozen and mobile lid cases, even though both show distributed strain in the lithosphere. The plate-like case is distinguished by an almost perfectly piecewise-constant horizontal velocity profile and by its remarkable stability in time.

ing plate-like behavior, a finding similar to that of *Tackley* [2000a], who has recently shown that a sublithospheric “asthenosphere” weakened due to partial melting is effective in producing plate-like behavior. We note, however, that partial melting may actually strengthen the mantle rather than weaken it [*Hirth and Kohlstedt*, 1996], whereas geophysical arguments for the existence of an LVZ based on observations do not constrain its cause or detailed geometry.

[9] All models have been run to secular equilibrium to characterize their behavior with respect to the LVZ viscosity contrast η^* and the yield stress σ_y . Model behavior is not strongly dependent on Rayleigh number [*Moresi and Solomatov*, 1998] (see, e.g., *Davies* [1986] for a definition), whose volume-averaged value for the models shown is $\sim 3 \times 10^8$. A model with $\sigma_y = 80$ MPa and $\eta^* = 1000$ is illustrated in Figure 2a (log viscosity) and 2b (temperature). The LVZ intrudes beneath spreading zones and is absent beneath convergence zones. Thermal heterogeneity for this snapshot is dominated

by two slowly migrating convergence zones. (The geotherm shown in Figure 1b is taken from this case, midway between zones of convergence and divergence.) Convection appears “normal” in Figure 2b, but the horizontal surface velocity profile in Figure 3 (solid green line) shows that the upper boundary layer is almost perfectly plate-like, with broad regions of constant velocity separated by highly localized zones of intense strain. This behavior is quite stable in time.

[10] Figure 2c shows the temperature contours for an otherwise identical case, but with increased $\sigma_y = 150$ MPa. Increased yield stress prevents failure of the upper boundary layer, rendering it immobile (Figure 3, dashed blue line). Small-scale convection occurs beneath the frozen lid. Figure 2d shows a case with $\eta^* = 1$ (no LVZ) and reduced $\sigma_y = 30$ MPa, yielding mobile lid behavior. The horizontal surface velocity profile shows isolated patches of constant velocity separated by broad zones of continuous deformation, and convection is very unsteady (chaotic).

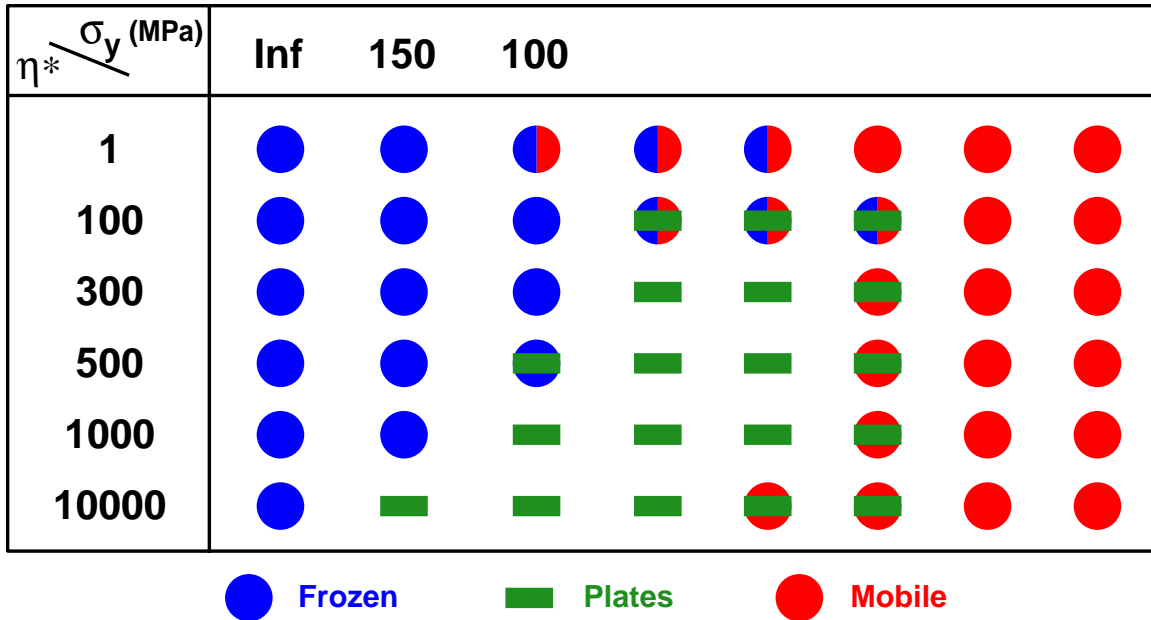


Figure 4. Character of upper boundary layer (lithosphere) motion (“frozen, plates, mobile”) as a function of yield stress and viscosity contrast for the 2-D numerical models. (Note that neither the vertical nor horizontal axes are linear in the model parameters.)

[11] A more complete perspective is obtained from the parameter space map in Figure 4, in which σ_y varies along rows and η^* varies along columns. For $\eta^* = 1$ (top row), we reproduce the results of *Moresi and Solomatov* [1998], with blue dots indicating the frozen lid regime, red dots a mobile lid, and split dots the transitional regime. (The somewhat plate-like solutions obtained recently in 3-D by *Trompert and Hansen* [1998] correspond to the latter transitional regime.) The results of *Weinstein and Olson* [1992], using a non-Newtonian lithosphere instead of viscoplastic failure, also correspond roughly to the results represented in the first row of Figure 4. As η^* increases, plate-like behavior fills the transitional regime (green bars). Composite symbols in Figure 4 indicate alternation among the different modes of behavior. The plate-like regime broadens (in terms of σ_y) with increasing η^* , verifying systematic stabilization of plate-like behavior by an LVZ for viscosity

contrasts 2 orders of magnitude and larger. Smaller viscosity contrasts may suffice for more severe forms of strain rate weakening in the lithosphere [*Bercovici*, 1993]. The development of a broad region of stable, plate-like behavior from a narrow zone of transitional behavior seen in Figure 4 is the main result of this paper and is consistent with the recent 3-D Cartesian results of *Tackley* [2000a]. We note that Tackley finds more plate-like behavior in 3-D geometry without an LVZ than is found for similar 2-D cases, suggesting that 3-D geometry also favors the formation of plates.

4. Spherical 3-D Model

[12] Do these 2-D results hold for 3-D spherical geometry? We have executed a case similar to the plate-like case shown in Figures 2a and 2b using a 3-D spherical version [*Yang*, 1997] of the same multigrid finite

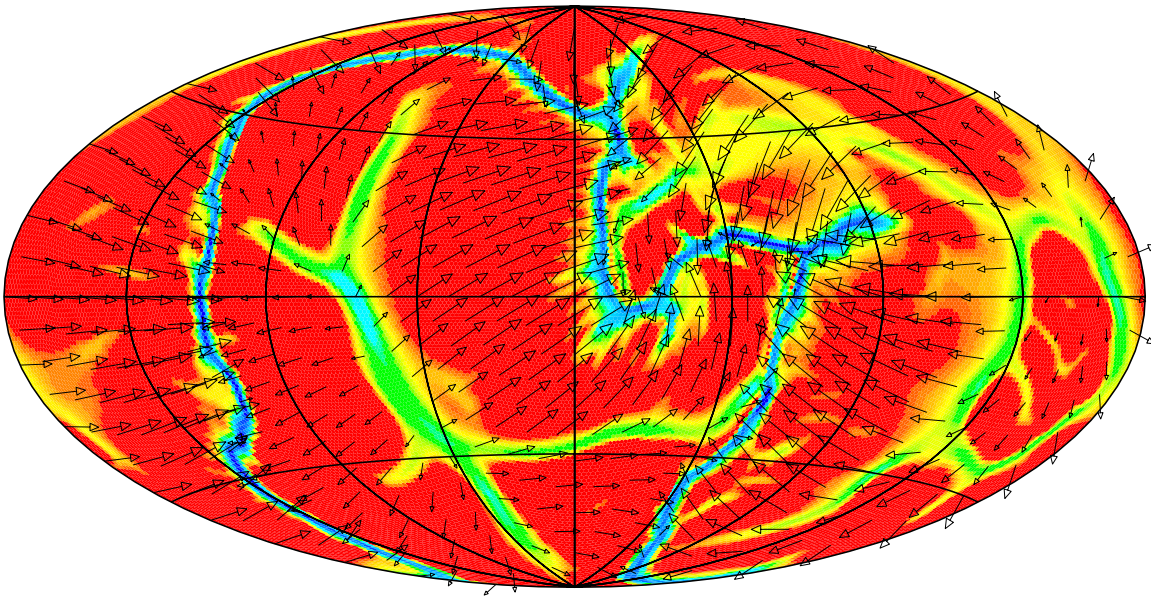


Figure 5. Surface planform of convection for the 3-D spherical calculation. The color contours are for log viscosity, with deepest blue corresponding to 10^{22} Pa-s and red corresponding to 3×10^{23} Pa-s. High strain rate zones (blue and green) separating plates show reduced viscosity due to plastic yielding. An LVZ (not shown) of viscosity contrast 1000 lies beneath the lithosphere. Arrows show the surface velocity field, which is plate-like in character. The largest arrows represent velocities of 8.3 cm/yr. Grid resolution is ~ 50 km (compared to 25 km for the 2-D models), which is the finest mesh we can run on the 128 processor Cray T3E. Finer resolution would allow us to model higher Rayleigh number convection and hence reduce the width of the weak zones between the plate-like regions. The reduction in Rayleigh number, relative to the 2-D models, is via an increase in specific heat, rather than by decreasing viscosity. For the 3-D model the radial viscosity variations defining the LVZ are smoother than for the 2-D models, with the sublithospheric reference viscosity reduced by a constant factor of 1000 from ~ 140 to 400 km depth relative to both the surface and to the lower mantle. The yield stress in this case is 140 MPa, a value that may have just yielded frozen lid behavior in the 2-D models (see Figure 4). Given that we are now in spherical geometry, that the Rayleigh number is reduced, and that the LVZ structure is smoother, it is not surprising that the yield stress range for plate-like behavior is shifted slightly.

element method. Heating is again internal, with strongly temperature-dependent viscosity and a plastic yield stress of 140 MPa for the lithosphere and 3 orders of magnitude viscosity reduction in a ~ 300 km thick LVZ beneath the lithosphere. The calculation was begun from random initial thermal perturbations (random spherical harmonic coefficients) and run for many overturn times (equivalent to ~ 2 billion years of Earth time) to secular equilibrium. The upper surface boundary condition was free-slip, as was the boundary

condition at the core-mantle boundary, throughout the run. The Rayleigh number is reduced about a factor of five from Earth-like values, due to computational limitations.

[13] Figure 5 shows log viscosity and surface velocities for the 3-D spherical model at secular equilibrium. The solution is very plate-like, with localized zones of high strain rate separating large regions of nearly constant angular velocities. Excluding net rotation, $\sim 30\%$ of the surface velocity field is toroidal motion,

characteristic of plate motions on a sphere and similar to Earth [Hager and O'Connell, 1978; Lithgow-Bertelloni *et al.*, 1993]. The internal thermal heterogeneity spectrum is peaked at spherical harmonic degree 2, also reflecting a pattern of flow similar to Earth [Su and Dziewonski, 1991]. Tackley [2000a] shows comparisons between cases with and without an LVZ in 3-D Cartesian geometry at modest Rayleigh number and demonstrates the increased "plate-ness" of surface motions induced by an LVZ. The 3-D spherical run shown in Figure 5 is mainly for demonstration and a more thorough exploration of parameter space in spherical geometry and at more Earthlike conditions (increased spatial resolution of plate "boundaries" and higher Rayleigh number) awaits the availability of considerably greater computational resources. Neither Tackley's nor our models give rise to transform-like plate boundaries, so that another piece of the rheological puzzle still remains elusive, probably owing to the isotropic nature of the failure law used so far in these convection models.

5. Discussion

[14] The mechanism by which an LVZ promotes plate tectonics is not entirely obvious. The LVZ reduces tractions on the base of the lithosphere, making plates less likely to deform except in established zones of failure. However, even without a plastic failure rheology, a low-viscosity upper mantle promotes a style of convection with widely separated linear downwellings [Bunge *et al.*, 1996], an effect that is not well-understood, and both mechanisms clearly contribute to plate-like behavior. It is important to recognize that it is not merely a weak zone beneath the plates that induces stable, plate-like behavior over a broad parameter range. In fact, models with strong but "breakable" plates over a weaker mantle fail in this regard, as is apparent from previous work [e.g., Weinstein and Olson, 1992; Moresi

and Solomatov, 1998]. Rather, plate-like behavior is promoted by a channel of low viscosity, or weakness, beneath a breakable lithosphere. In fact, cases we have run with much narrower LVZ's exhibit plate-like behavior just as readily as those summarized in Figure 4.

[15] Several cautions are in order before applying the results of this study: First, our viscoplastic failure law causes plate boundary formation in response to instantaneous local stresses. In reality, Earth's plate boundaries appear to persist indefinitely as weak zones, as ancient plate boundaries are commonly reactivated during plate motion rearrangements [e.g., Gurnis *et al.*, 2000]. The values of σ_y for which we obtain plate-like behavior (50–150 MPa) are reasonable for Earth's lithosphere [Brace and Kohlstedt, 1980]. However, major established fault zones may be weaker (10–20 MPa) [Lachenbruch and Sass, 1980; Zoback *et al.*, 1987], and other failure laws may better describe the formation and persistence of plate boundaries. The values of η^* and the thickness of the LVZ channel we have used are larger than some estimates [Hager and Richards, 1989; Mitrovica, 1996], so it will be important to determine how different lithospheric failure mechanisms affect the LVZ characteristics required for plate-like behavior to occur. We also note that our models are applicable mainly to Earth's oceanic lithosphere and do not account for the effects of continental lithosphere and crust on plate tectonics. The fact that much subduction of oceanic lithosphere occurs along continental margins, the likelihood that the LVZ is greatly diminished, if not completely absent, beneath continental lithosphere [Ricard *et al.*, 1991], and the fact that plate tectonics often does not apply to continental interiors all suggest avenues for more sophisticated modeling work in the future.

[16] With these qualifications in mind our results suggest the following qualitative interpretation of the tectonic styles of Venus, Earth,

Table A1. Nusselt Number Benchmark Results for Spherical Mantle Convection Models^a

Ra Number	TERRA	TR	DB	GG	HH	CitcomS
7,000	3.4160	3.4423	3.4657	NA	3.4957	3.5190
14,000	4.2250	4.2028	NA	4.2820	4.2818	NA

^aTR from *Ratcliff et al.* [1996]; DB from *Bercovici et al.* [1989]; GG from *Glatzmaier* [1988]; HH from *Harder and Christensen* [1996]; CitcomS from *Zhong et al.* [2000]. The values given are Nusselt number for a steady tetrahedral ($L = 3$, $m = 2$) pattern of convection in a spherical shell of inner radius 3000 km and outer radius 6000 km. Flow is incompressible and the shell is heated entirely from below. The Ra number = 14,000 case is the more “stringent” test, although much higher Ra number values need to be tested in the future. The codes, which use a variety of numerical techniques, agree within a few percent, which is generally considered to be acceptable for 3-D calculations.

and Mars: Mars is a frozen lid planet. Earth is dominated by a plate tectonic style of convection due to a pronounced LVZ and weak fault zones in the lithosphere, both of which may be related to the presence of water in the upper mantle and crust [*Hirth and Kohlstedt*, 1996; *Karato and Jung*, 1998; *Brace and Kohlstedt*, 1980]. Venus, whose composition and size are similar to Earth, may be transitional between mobile and frozen regimes, with possible episodic overturn of its lithosphere [*Strom et al.*, 1994], or is perhaps in the frozen regime, with episodic volcanic resurfacing [*Reese et al.*, 1999]. Venus lacks both free water and an LVZ, which may explain its lack of plate tectonics [*Phillips*, 1990; *Solomon et al.*, 1991; *Kaula*, 1990, 1995]. Recycling of volatiles at subduction zones may hydrate Earth’s upper mantle, in turn promoting plate tectonics (and subduction), suggesting a potentially important feedback mechanism.

Appendix A. Notes on Validation of Numerical Methods

[17] The 2-D code used in this study was benchmarked for constant viscosity convection in *Travis et al.* [1990], and the variable viscosity version of the code is described in detail by *Yang and Baumgardner* [2000]. No 2-D benchmark exists for the strong viscosity variations and high Rayleigh numbers treated in this paper, although the general agreement of our results with those of *Tackley* [2000a] may

be considered as a qualitative benchmark at these extreme conditions.

[18] The 3-D spherical code TERRA was benchmarked for constant viscosity convection by *Bunge* [1997], who found good agreement (1.5% or less differences) with the results of *Glatzmaier* [1988] for Nusselt number, peak velocities, and peak temperatures. Table A1 summarizes the Nusselt number results for two standard 3-D spherical convection cases that have been computed by a number of authors:

[19] These benchmark cases are for relatively low Rayleigh number, and there are no time-dependent or variable viscosity benchmarks (of which we are aware) for 3-D spherical convection. The variable viscosity formulation of TERRA is described by *Yang* [1997]. The accuracy of the multigrid momentum solver for TERRA was demonstrated by *Baumgardner and Frederickson* [1985], who compared numerical solutions of the Poisson equation on the sphere with analytical solutions. The momentum solver also gives excellent (<2% error for harmonic degrees 1–8) agreement with analytical solutions [*Hager and O’Connell*, 1981] for instantaneous poloidal flow generated by internal density anomalies. Efforts are underway within the geodynamics community to establish a set of benchmarks for high Rayleigh number, variable viscosity convection.

Acknowledgments

[20] This work was supported by grants from NSF, NASA, and the Institute of Geophysics and Planetary Physics (IGPP) at Los Alamos National Laboratory. We thank Shun Karato, Mike Gurnis, Norm Sleep, Slava Solomatov, Paul Tackley, Stuart Weinstein, Yanick Ricard, Rick O'Connell, and three anonymous reviewers for constructive comments on the manuscript.

References

- Alcouffe, R. E., A. Brandt, J. E. Dendy Jr., and J. W. Painter, The multi-grid method for the diffusion equation with strongly discontinuous coefficients, *SIAM J. Sci. Stat. Comput.*, **2**, 430–454, 1981.
- Baumgardner, J. R., and P. O. Frederickson, Icosahedral discretization of the two sphere, *SIAM, J. Numer. Anal.*, **22**, 1107–1115, 1985.
- Bercovici, D., A simple model of plate generation from mantle flow, *Geophys. J. Int.*, **114**, 635–650, 1993.
- Bercovici, D., G. Schubert, and G. A. Glatzmaier, Three-dimensional spherical models of convection in the Earth's mantle, *Science*, **244**, 893–1016, 1989.
- Brace, W. F., and D. L. Kohlstedt, Limits on lithospheric stress imposed by laboratory experiments, *J. Geophys. Res.*, **85**, 6248–6252, 1980.
- Bunge, H.-P., M. A. Richards, and J. R. Baumgardner, The effect of depth-dependent viscosity on the planform of mantle convection, *Nature*, **379**, 436–438, 1996.
- Bunge, H.-P., Numerical models of mantle convection, Ph.D. thesis, Univ. of Calif., Berkeley, 1997.
- Cathles, L. M., *The Viscosity of the Earth's Mantle*, Princeton Univ. Press, Princeton, N. J., 1975.
- Christensen, U. R., Convection with pressure and temperature dependent non-Newtonian rheology, *Geophys. J. R. Astron. Soc.*, **77**, 343–384, 1984.
- Davies, G. F., Mantle convection under simulated plates: Effects of heating modes and ridge and trench migration, and implications for the core-mantle boundary, bathymetry, the geoid and Benioff zones, *Geophys. J. R. Astron. Soc.*, **84**, 153–183, 1986.
- Glatzmaier, G. A., Numerical simulations of mantle convection: Time-dependent, three-dimensional, compressible, spherical shell, *Geophys. Astrophys. Fluid Dyn.*, **43**, 223–264, 1988.
- Grand, S. P., and D. V. Helmberger, Upper mantle shear structure beneath the northwest Atlantic Ocean, *J. Geophys. Res.*, **89**, 11,465–11,475, 1984.
- Gurnis, M., S. Zhong, and J. Toth, On the competing roles of fault reactivation and brittle failure in generating plate tectonics from mantle convection, in *The History and Dynamics of Plate Motion*, *Geophys. Monogr. Ser.*, vol. 121, edited by M. A. Richards, R. Gordon, and R. D. van der Hilst, pp. 73–94, AGU, Washington, D. C., 2000.
- Hager, B. H., and R. J. O'Connell, Kinematic models of large-scale flow in the Earth's mantle, *J. Geophys. Res.*, **84**, 1031–1048, 1978.
- Hager, B. H., and R. J. O'Connell, A simple model of plate dynamics and mantle convection, *J. Geophys. Res.*, **86**, 4843–4878, 1981.
- Hager, B. H., and M. A. Richards, Long-wavelength variations in Earth's geoid: Physical models and dynamical implications, *Philos. Trans. R. Soc. London, Ser. A*, **328**, 309–327, 1989.
- Hales, A. L., J. R. Cleary, H. A. Doyle, R. Green, and J. Roberts, *P*-wave station anomalies and structure of the upper mantle, *J. Geophys. Res.*, **73**, 3885–3895, 1968.
- Harder, H., and U. R. Christensen, A one-plume model of Martian mantle convection, *Nature*, **380**, 507–509, 1996.
- Hirth, G., and D. L. Kohlstedt, Water in the oceanic upper mantle: Implications for rheology, melt extraction and the evolution of the lithosphere, *Earth Planet. Sci. Lett.*, **144**, 93–108, 1996.
- Karato, S.-I., and H. Jung, Water, partial melting and the origin of the seismic low velocity and high attenuation zone in the upper mantle, *Earth Planet. Sci. Lett.*, **193**, 193–207, 1998.
- Karato, S. I., and P. Wu, Rheology of the upper mantle: A synthesis, *Science*, **260**, 771–778, 1993.
- Kaula, W. M., Venus: A contrast in evolution to Earth, *Science*, **247**, 1191–1196, 1990.
- Kaula, W. M., Venus reconsidered, *Science*, **270**, 1460–1464, 1995.
- King, S. D., C. W. Gable, and S. Weinstein, Models of convection driven tectonic plates: A comparison of methods and results, *Geophys. J. Int.*, **109**, 481–487, 1992.
- Lachenbruch, A. H., and J. H. Sass, Heat flow and energetics of the San Andreas fault zone, *J. Geophys. Res.*, **85**, 6185–6222, 1980.
- Lithgow-Bertelloni, C. L., M. A. Richards, Y. Ricard, R. J. O'Connell, and D. C. Engebretson, Toroidal-poleoidal partitioning of plate motion since 120 Ma, *Geophys. Res. Lett.*, **20**, 357–378, 1993.
- Mitrovica, J. X., Haskell [1935] revisited, *J. Geophys. Res.*, **101**, 555–569, 1996.
- Moresi, L., and V. Solomatov, Mantle convection with a brittle lithosphere: Thoughts on the global tectonic styles of the Earth and Venus, *Geophys. J. Int.*, **133**, 669–682, 1998.
- Phillips, R. J., Convection-driven tectonics on Venus, *J. Geophys. Res.*, **95**, 1301–1316, 1990.
- Ratcliff, J. T., G. Schubert, and A. Zebib, Steady tetrahe-

- dral and cubic patterns of spherical-shell convection with temperature-dependent viscosity, *J. Geophys. Res.*, *101*, 25,473–25,484, 1996.
- Reese, C. C., V. S. Solomatov, and L.-N. Moresi, Non-Newtonian stagnant lid convection and magmatic resurfacing on Venus, *Icarus*, *139*, 67–80, 1999.
- Ricard, Y., C. Doglioni, and R. Sabadini, Differential rotation between lithosphere and mantle: A consequence of lateral mantle viscosity variations, *J. Geophys. Res.*, *96*, 8407–8415, 1991.
- Solomon, S. C., et al., Venus tectonics: initial analysis from Magellan, *Science*, *252*, 297–312, 1991.
- Strom, R. G., G. G. Scaber, and D. D. Dawson, The global resurfacing of Venus, *J. Geophys. Res.*, *99*, 10,899–10,926, 1994.
- Su, W.-J., and A. M. Dziewonski, Predominance of long-wavelength heterogeneity in the mantle, *Nature*, *352*, 121–126, 1991.
- Tackley, P. J., Self-consistent generation of tectonic plates in time-dependent, three-dimensional mantle convection simulations, 2, Strain weakening and asthenosphere, *Geochem. Geophys. Geosyst.*, vol. 1, Paper number 2000GC000043 [14,420 words, 15 figures, 1 table], 2000a. (Available at <http://www.g-cubed.org/publicationsfinal/articles/2000GC000043/fs2000GC000043.html>)
- Tackley, P. J., The quest for self-consistent incorporation of plate tectonics in mantle convection, in *The History and Dynamics of Plate Motion*, *Geophys. Monogr. Ser.*, vol. 121, edited by M. A. Richards, R. Gordon, and R. D. van der Hilst, pp. 47–72, AGU, Washington, D. C., 2000b.
- Travis, B. J., C. Anderson, J. Baumgardner, C. W. Gable, B. H. Hager, R. J. O'Connell, P. Olson, A. Raefsky, and G. Schubert, A benchmark comparison of numerical methods for infinite Prandtl number thermal convection in two-dimensional Cartesian geometry, *Geophys. Astrophys. Fluid Dyn.*, *55*, 137–160, 1990.
- Trompert, R., and U. Hansen, Mantle convection simulations with rheologies that generate plate-like behavior, *Nature*, *395*, 686–689, 1998.
- Weinstein, S. A., Thermal convection in a cylindrical annulus with a non-Newtonian outer surface, *Pure Appl. Geophys.*, *146*, 551–572, 1996a.
- Weinstein, S. A., The potential role of a non-Newtonian rheology in the resurfacing of Venus, *Geophys. Res. Lett.*, *23*, 511–514, 1996b.
- Weinstein, S. A., and P. L. Olson, Thermal convection with non-Newtonian plates, *Geophys. J. Int.*, *111*, 515–530, 1992.
- Yang, W.-S., Variable viscosity thermal convection at infinite Prandtl number in a thick spherical shell, Ph.D. thesis, Univ. of Ill., Urbana, 1997.
- Yang, W.-S., and J. R. Baumgardner, A matrix-dependent transfer multigrid method for strongly variable viscosity infinite Prandtl number thermal convection, *Geophys. Astrophys. Fluid Dyn.*, in press, 2000.
- Zhong, S., M. Gurnis, and L. Moresi, Role of faults, nonlinear rheology, and viscosity structure in generating plates from instantaneous mantle flow models, *J. Geophys. Res.*, *103*, 15,255–15,268, 1998.
- Zhong, S., M. T. Zuber, L. Moresi, and M. Gurnis, Role of temperature-dependent viscosity and surface plates in spherical shell models of mantle convection, *J. Geophys. Res.*, *105*, 11,063–11,082, 2000.
- Zoback, M. D., et al., New evidence on the state of stress of the San Andreas fault system, *Science*, *238*, 1105–1111, 1987.